

## Dense and Sparse Vortices in Excitable Media Drift in Opposite Directions in Electric Field

V. Krinsky, E. Hamm, and V. Voignier

*Institut Non Linéaire de Nice, 1361 Route des Lucioles, 06560 Valbonne, France*

(Received 20 July 1995)

Two mechanisms for vortex drift in an advective field are described. The velocity of vortex tip movement in an advective field is periodically modulated. It results in the periodical modulations of the core size of the vortex. While periodical changes of the core size (mechanism 1) result in vortex drift parallel to the electric field, periodical changes of the velocity (mechanism 2) result in the vortex drift in the opposite direction. Mechanism 1 dominates in sparse vortices, mechanism 2 dominates in dense vortices. Arguments used to predict the effect suggest its generic nature. [S0031-9007(96)00199-8]

PACS numbers: 82.20.Mj, 66.30.Qa, 82.20.Wt

The dynamics of rotating waves (vortices) in excitable media can be affected by an electric field [1–4]. A constant electric field induces drift of the vortices [2,3]. The component of the drift perpendicular to the electric field changes its sign with the chirality of the vortex [5]. The component of the drift parallel to the field is not affected by change in the chirality. For example, in the Belousov-Zhabotinsky (BZ) chemical excitable media, the vortices are known to always drift towards the positive electrode [2,3,6]. The physical mechanism of the drift seems straightforward: ionic components are involved, which are moved by electric field. If the key component is negatively charged, it moves to the positive electrode (antiparallel to the electric field) thus inducing a displacement of the wave pattern (with possible deformation and a perpendicular component of drift for chiral structures). We have found that essential features are missing in this picture. Dense and sparse vortices drift in opposite directions even in the simplest case when advective electric field affects activator only. For a positive advection coefficient, the dense vortex drifts towards the positive electrode, while the sparse vortex drifts to the negative one.

(1) *The model.*—We analyze the effect of electric field  $E$  on spiral dynamics for the case where  $E$  affects activator,  $U$ , only, and  $E$  is directed parallel to the  $X$  axis (Fig. 1):

$$U_t = \epsilon^{-1} f(U, V) + D_1 \nabla^2 U + M_1 E U_X, \quad (1)$$

$$V_t = \psi(U, V) + D_2 \nabla^2 V. \quad (2)$$

Here, functions  $f$  and  $\psi$  describe local kinetics (e.g., Barkley's model [7]:  $f(U, V) = U(1 - U)[U - (V + b)/a]$ ,  $\psi(U, V) = U - V$ ),  $\epsilon \ll 1$ . The second terms in (1) and (2) describe diffusion, and the last term in (1) describes advection. It is a generic case: If the field affects both activator  $U$  and inhibitor  $V$ ,

$$U_t = \epsilon^{-1} f(U, V) + D_1 \nabla^2 U + M_1 E U_X, \quad (3)$$

$$V_t = \psi(U, V) + D_2 \nabla^2 V + M_2 E V_X, \quad (4)$$

then by changing to a moving frame  $x_1 = x + M_2 E t$ , one arrives at Eqs. (1) and (2) with rescaled  $M'_1 = M_1 - M_2$ .

(2) *Effect of electric field on wave propagation.*—For  $M_1 = M_2$ , the advection terms can be removed in the moving frame  $x_1 = x + M_1 E t$ . This means that in the laboratory frame the following hold: (1) In 1D, the velocity  $C_+$  of pulses propagating antiparallel to  $E$  (to the positive electrode) is larger than the velocity  $C_-$  of pulses propagating in the opposite direction ( $M_1 > 0$  is supposed)

$$C_+ = C_0 + M_1 E, \quad C_- = C_0 - M_1 E \quad (5)$$

as found in experiments with chemical excitable media [8,9]. (2) In 2D, a drift of the spiral wave is induced

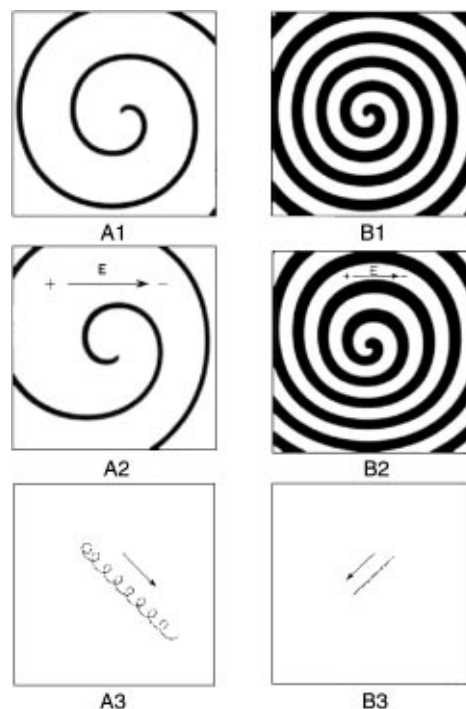


FIG. 1. Sparse (A) and dense (B) vortices. Excited state ( $u > 0.5$ ) is shown in black: (1) without electric field; (2) with an electric field  $E = 0.35$  (shown by arrow). Note deformation of the spiral. (3) Trajectories of vortex tip movement. Parameters are  $\epsilon = 0.02$ ,  $D_1 = 1$ ,  $D_2 = 0$ ,  $L = 80$ , grid  $256 \times 256$  points,  $dt = 0.00244$ , in A:  $a = 0.55$ ,  $b = 0.05$ ; in B:  $a = 1.0$ ,  $b = 0.03$ .

by  $E$ . The drift velocities,  $C_{\parallel}$  parallel to  $E$ , and  $C_{\perp}$  perpendicular to  $E$ , are

$$C_{\parallel} = M_1 E, \quad C_{\perp} = 0. \quad (6)$$

It means also that there is no deformation of the spiral wave. For  $M_1 \neq M_2$  in (3) and (4) this is not the case: the spiral is deformed and  $C_{\perp} \neq 0$  [10]. Generically  $C_{\perp} \neq 0$  for an arbitrary wave configuration which is not symmetric with respect to reflections  $Y = -Y$ .

Change of chirality of the spiral changes the sign of perpendicular velocity  $C_{\perp}$  [5]. The direction of the drift can be changed trivially, by changing the sign of the advection term  $M_1 E U_X$  in Eq. (1). No other mechanisms of changing the sign of drift velocity are known.

(3) *Dense and sparse spiral waves.*—Spiral waves with  $\lambda_e/\lambda \ll 1$ , we call sparse, or loose spirals [Fig. 1(A)], contrary to dense, or tight spirals where  $\lambda_e/\lambda \lesssim 1$  [Fig. 1(B)]:

$$\lambda_e/\lambda \ll 1 \text{ sparse spirals}, \quad \lambda_e/\lambda \lesssim 1 \text{ dense spirals}. \quad (7)$$

Here,  $\lambda$  is wavelength (pitch) of the spiral, and  $\lambda_e$  (shown in black in Fig. 1) is the excitation wavelength

$$\lambda_e = C\tau, \quad (8)$$

where  $C$  is the velocity and  $\tau$  is a characteristic duration of the pulse.

Different physical mechanisms control these spiral waves. For dense spirals, the interaction of a wave with the previous one is important, while for sparse spiral waves it is not the case. The curvature of the wave near the tip selects the wavelength  $\lambda$  of the sparse spiral. Changing parameters one can induce a smooth transition from sparse to dense spirals. In Barkley's model, it can be achieved, e.g., by decreasing parameter  $b$  or by increasing parameter  $a$ . In this way, one also diminishes radius  $r$  of the core and period  $T$  of a spiral wave.  $T, \lambda, r$  are limited from below by  $\infty > T > T_{\min} \sim \tau$ ,  $\infty > \lambda > \lambda_{\min} \sim C\tau$ ,  $\infty > r > r_{\min} \sim C\tau/2\pi$ .

(4) *Spiral waves in electric field.*—Below we describe two mechanisms causing drift of the vortex in opposite directions. When a wave rotates in an electric field, the normal velocity  $C$  changes periodically: it increases when the wave propagates to the positive electrode, and decreases when it moves in the opposite direction [Eq. (5)]. The same is true for the excitation wavelength  $\lambda_e$  [Eq. (8)].

*Mechanism (1): Periodical changes of the core size.*—Increase in  $\lambda_e$  results in a smaller core (Fig. 3). The radius  $r$  of the core changes periodically, diminishing when the vortex tip moves towards the positive electrode, and increasing when the tip moves towards the negative one. This results in a vortex drift towards the *negative* electrode [Fig. 2(A1)]. Mechanism (1) is more pronounced in *sparse* vortices.

*Mechanism (2): Periodical changes of the propagation velocity.*—For *dense* vortices, a small change in  $\lambda_e =$

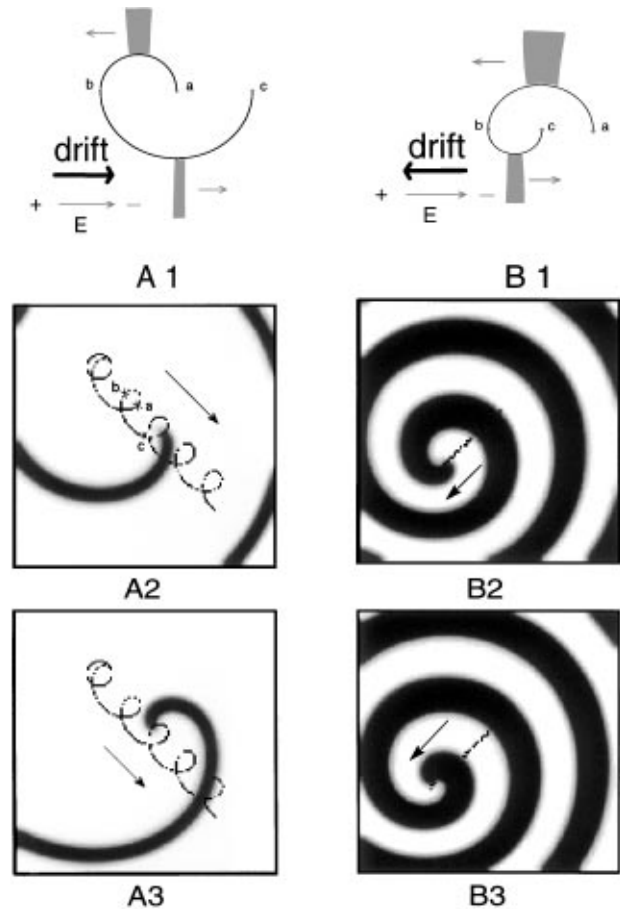


FIG. 2. Mechanism of drift of sparse (A) and dense (B) vortices in electric field: (1) schematic, (2),(3) computer simulations. The arrow in frames (2),(3) indicates the drift direction. Wave tip propagates: (2) parallel to  $E$ , (3) antiparallel to  $E$  (half a period later). Note that the tip width  $\lambda_e$  (near the arrow) in B2 is thin, and in B3 is thick. Same parameters as in Fig. 1, except  $L = 40, 128 \times 128$  points.

$C\tau$  cannot significantly affect the core radius  $r$  (Fig. 3). During the first half of the period, the vortex tip moves to the positive electrode with an increased velocity ( $\sim C_+$ ), and during the next half of the period it moves to the negative electrode with a decreased velocity ( $\sim C_-$ ). It results in drift towards the *positive* electrode [Fig. 2B1].

How does variation of parameters affect the core size of the spiral? Movement of the tip of a spiral wave is characterized by two velocities: normal velocity  $C_n$ , and tangential, or growing, velocity  $C_g$ . The growing velocity  $C_g$  is important: If  $C_g < 0$ , a wave segment contracts in length, and a rotating wave is destroyed [11,12]. There is no theoretical understanding of growing velocity  $C_g$ .

On the other hand, from a topological point of view, a rotating wave is equivalent to a dislocation type defect in a striped pattern (e.g., in a lattice, or in a liquid crystal). There is also a geometrical analogy. In a polar coordinate system, with the origin in the center of the spiral core, the equation of a steadily rotating spiral can be written as

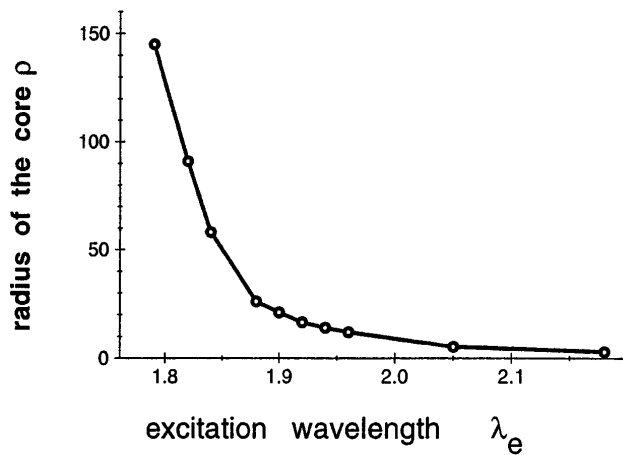


FIG. 3. Dependence of core size on  $\lambda_e$ . Parameters:  $E = 0$ ,  $L = 40$ ,  $128 \times 128$  points,  $a = 0.53$ ,  $b = 0.05$ .

$\phi = \phi_0(\rho) + \omega t$ , where  $\omega$  is the angular velocity of the spiral rotation. A change of variables [13]

$$\rho \rightarrow \rho, \quad \phi \rightarrow \phi - \phi_0(\rho) - \omega t, \quad (9)$$

makes the angle  $\phi$  constant along the whole wave. The spiral wave is converted into a straight line, and the wave tip becomes a dislocation. Movement of dislocations is well understood via dislocation theory [14,15]. This analogy may be useful in future development of the theory. Now we just mention that for both rotating spirals and dislocations, a critical value of a control parameter exists such that if  $\alpha \rightarrow \alpha_0$  the growing velocity  $C_g \rightarrow 0$ . For rotating spirals, it is an indication that the core size diverges.

In Fig. 3, the dependence of the core size on  $\lambda_e$  is shown, obtained numerically for Eqs. (1) and (2). It is seen that the core size infinitely grows when  $\lambda_e \rightarrow \lambda_e^0 \approx 1.79$ . At  $\lambda_e \approx \lambda_e^0$ , a sparse vortex is observed; the sensitivity of its core size to the variation of  $\lambda_e$  is high. At larger values of  $\lambda_e$ , the vortex becomes less sparse; the sensitivity of its core size to the variations of  $\lambda_e$  is reduced. This underlies the difference between mechanisms (1) and (2).

For mechanism (1), the vortex tip trajectory  $bc$  [Fig. 2(A1)] is formed by a large core, with radius  $r \sim r_-$  corresponding to the smaller  $\lambda_{e-} = C_- \tau$ . The trajectory  $ab$  is formed by a smaller core, with radius  $r \sim r_+$  corresponding to the larger  $\lambda_{e+} = C_+ \tau$ . The vortex drift velocity for mechanism (1) is  $C_{d1} = 2 \langle r_- - r_+ \rangle T^{-1}$ , where  $\langle \dots \rangle$  is an averaging over the angular variable. For mechanism (2), the drift velocity is  $C_{d2} = 0.5 \langle C_+ - C_- \rangle$  [Fig. 2(B1)]. The resulting drift velocity created by the two simultaneously operating mechanisms  $C_d = C_{d1} - C_{d2}$  is of opposite sign for dense and sparse vortices.

The dependence of the vortex drift velocity on parameters obtained numerically using the program [7] is shown

in Fig. 4. For parameter values where displacements due to mechanisms (1) and (2) were balanced ( $a \sim 0.97$ ), there was no displacement of the vortex in the direction of the electric field ( $C_{\parallel} = 0$ ,  $C_{\perp} \neq 0$ ). The sign of the perpendicular velocity  $C_{\perp}$  was not changed.

Drift of a spiral wave in the electric field was analyzed in [16]. No opposite directions of drift were found because developed theory exists only for small core [17], i.e., for dense vortices. Kinematical models [18] are successful in using curvature effects to describe the normal velocity of sparse vortices, but the description of growing (tangential) velocity  $C_g$  is based on phenomenologically adjusted parameters. There is no satisfactory theory for sparse vortices. The effects found in our Letter may also be present in solutions to the Ginzburg-Landau equations, where the vortices are well understood [19,20].

The effect predicted here can be observed in excitable media governed by Eqs. (1) and (2) but not in those governed by Eqs. (3) and (4). Although Eqs. (1) and (2) are generic, and Eqs. (3) and (4) are reduced to (1) and (2) in a moving frame  $x_1 = x + vt$  where  $v = M_2 E$ , but when coming back to the laboratory frame, all velocities  $C$

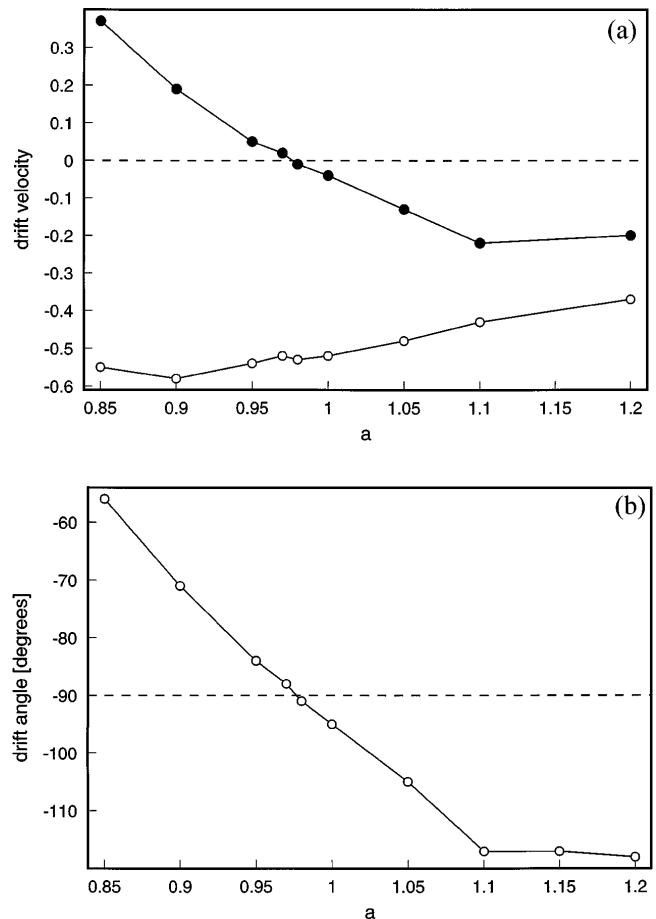


FIG. 4. Dependence of the (a) drift velocity and (b) angle on the parameter  $a$  ( $b = 0.13$ ). Empty circles:  $C_{\perp}$ , filled circles:  $C_{\parallel}$ .

will be modified:  $C_{\text{lab}} = C - v$ . For  $v > C$ , velocities  $C_{\text{lab}}$  will become of the same sign although velocities  $C$  were of different signs. This is typical for the BZ reaction in a solution because the diffusion coefficients are of the same order, and the mobilities  $M_i$  are proportional to the diffusion coefficients  $D_i$ :

$$M_i = (F/RT)z_i D_i, \quad (10)$$

where  $F$  is the Faraday constant,  $R$  is the gas constant, and  $z$  is the charge number. An immobilization of some of the reagents will help to avoid this difficulty.

For biological excitable media, there is no such difficulty, because only a diffusion coefficient  $D_1 \neq 0$ , and  $D_2 = D_3 = \dots = D_n = 0$ , where  $k = n - 1$  is the dimension of vector  $V$  ( $k = 3$  in Hodgkin-Huxley equations). Each component of  $V$  describes opening or closing of ionic channels for different ions. They are governed by local voltages only and do not diffuse [21].

We benefited from discussions with L. Gil, A. Pumir, S. Rica, A. Belmonte, and J. M. Flesselles.

- 
- [1] V. Perez-Munuzuri *et al.*, *Nature* (London) **353**, 740 (1991).  
 [2] K. Agladze and P. D. Kepper, *J. Phys. Chem.* **96**, 5239 (1992).  
 [3] O. Steinbock, J. Schutze, and S. Muller, *Phys. Rev. Lett.* **68**, 248 (1992).

- [4] A. P. Munuzuri *et al.*, *Phys. Rev. E* **50**, 4258 (1994).  
 [5] A. P. Munuzuri *et al.*, *Phys. Rev. E* **48**, 3232 (1993).  
 [6] A. Belmonte and J.-M. Flesselles, *Europhys. Lett.* **32**, 267 (1995).  
 [7] D. Barkley, *Physica* (Amsterdam) **49D**, 61 (1991).  
 [8] H. Sevcikova and M. Marek, *Physica* (Amsterdam) **9D**, 140 (1983).  
 [9] P. Ortoleva, *Nonlinear Chemical Waves* (J. Wiley, New York, 1992).  
 [10] E. Hamm, J. M. Flesselles, and E. Tirapegui, INLN report, 1995 (to be published).  
 [11] V. S. Zykov, *Simulation of Wave Processes in Excitable Media* (Manchester Univ. Press, Manchester, 1987).  
 [12] E. Meron and P. Pelce, *Phys. Rev. Lett.* **60**, 1880 (1988).  
 [13] J. M. Greenberg, *SIAM J. Appl. Math.* **30**, 199 (1976).  
 [14] L. Landau and E. Lifchitz, *Theorie de l'Elasticite* (Mir, Moscow, 1967), p. 165.  
 [15] M. Kleman, *Points, Lignes, Parois* (Les Editions de Physique, Paris, 1977), p. 152.  
 [16] I. Mitkov, I. Aranson, and D. Kessler, *Phys. Rev. E* **52**, 5974 (1995).  
 [17] D. Kessler, H. Levine, and W. Reynolds, *Phys. Rev. Lett.* **68**, 401 (1992).  
 [18] A. Mikhailov, V. Davydov, and V. Zykov, *Physica* (Amsterdam) **70D**, 1 (1994).  
 [19] P. Couillet, L. Gil, and J. Lega, *Phys. Rev. Lett.* **62**, 1619 (1989).  
 [20] P. Couillet, L. Gil, and J. Lega, *Physica* (Amsterdam) **37D**, 91 (1989).  
 [21] A. L. Hodgkin and A. F. Huxley, *J. Physiol.* **117**, 500 (1952).